

# Experimental demonstration of lossy mode and surface plasmon resonance generation with Kretschmann configuration

IGNACIO DEL VILLAR,<sup>1,\*</sup> VICTOR TORRES,<sup>1</sup> MIGUEL BERUETE<sup>1</sup>

<sup>1</sup> Electrical and Electronic Engineering Department, Public University of Navarra, 31006 Pamplona, Spain

\*Corresponding author: [ignacio.delvillar@unavarra.es](mailto:ignacio.delvillar@unavarra.es)

Received XX Month XXXX; revised XX Month, XXXX; accepted XX Month XXXX; posted XX Month XXXX (Doc. ID XXXXX); published XX Month XXXX

**Lossy mode resonances (LMRs) and surface plasmon resonances (SPRs) are obtained experimentally with a Kretschmann configuration using a BK7 glass prism with all sides polished and coated with Indium Tin Oxide (ITO). The properties of ITO permit to obtain LMRs and SPRs with the same experimental set-up. The results are corroborated with a numerical method for calculation of the reflection in the Kretschmann configuration. © 2015 Optical Society of America**

**OCIS codes:** (310.0310) Thin-films, (240.6680) Surface plasmons, (130.6010) Sensors, (310.7005) Transparent conductive coatings.

<http://dx.doi.org/10.1364/OL.99.099999>

During the last decades a lot of research has been dedicated to surface plasmon resonances (SPRs) and lossy mode resonances (LMRs), due to their applicability in the field of sensors [1–7]. Compared to SPRs, LMRs present some interesting properties such as the excitation under both TE and TM polarization, the ability to generate several resonances in the same spectrum and the easy control of the position of the resonance in the optical spectrum by increasing the thin-film thickness [5–8].

Moreover, in contrast with SPRs, the materials that support LMRs have a low imaginary part of the refractive index and therefore are non-metallic. This can be explained by taking into account the conditions necessary for obtaining each resonance. For SPRs the real part of the thin-film permittivity must be negative and larger in magnitude than both its own imaginary part and the real part of the permittivity of the material surrounding the thin-film. However, for LMRs the real part of the thin-film permittivity must be positive and larger in magnitude than both its own imaginary part and the real part of the permittivity of the material surrounding the thin-film [9]. In this respect, indium tin oxide (ITO) is an interesting solution since it satisfies both the conditions for LMR generation at short wavelengths [5,10], and the conditions for generation of SPRs at long wavelengths [11]. Therefore, it allows having both types of resonances in a single structure.

Several works have already shown the possibility to obtain SPRs with an ITO thin-film in a Kretschmann configuration [11,12]. On the other hand, LMRs have only been demonstrated experimentally using ITO coated optical fiber [5,8], while the phenomenon with a Kretschmann configuration has only been proved theoretically [7,10]. The main reason for this is that SPRs are obtained typically for angles ranging between 40° and 70° [11], whereas LMRs arise typically at near-

grazing angle incidence, i.e. angles approaching 90°, which are adequate for optical fiber excitation [10]. Consequently, LMRs cannot be excited with an equilateral prism or a right-angle prism if light is not directed onto the lateral sides. Unfortunately, commercial prisms are not polished on the lateral sides, preventing their utilization for LMR generation.

In this letter we tackle this problem by using a right angle prism with all its sides polished, specifically designed for this purpose. By using this prism, we demonstrate both theoretically and experimentally LMR excitation with a Kretschmann configuration. Moreover, the same experimental setup allows us to excite SPRs by simply varying the incidence angle. So, in a single configuration setup, we are able to control independently two resonances, opening the path for enhanced sensing applications. In Fig. 1 the experimental setup is depicted.

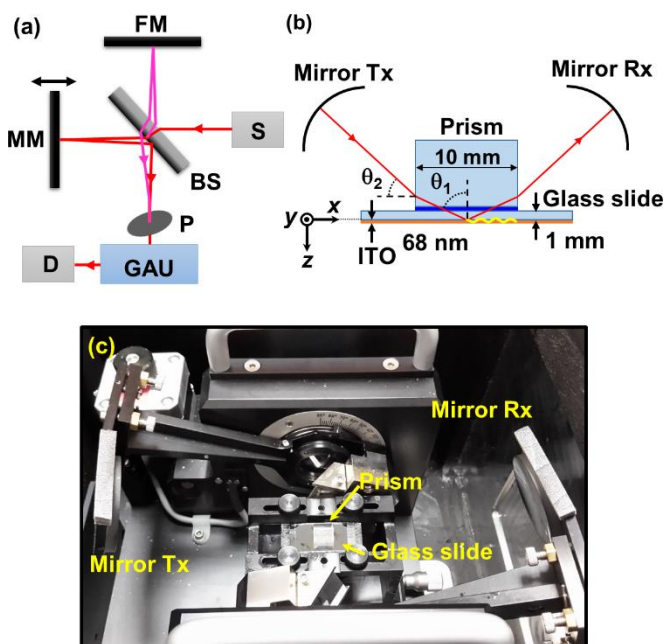


Fig. 1. (a) Schematic of the FTIR with the following elements: S: source, BS: beamsplitter, FM: fixed mirror, MM: movable mirror, P: polarizer, GAU: grazing angle unit, D: detector. (b) Sketch of the experimental setup showing the prism laying on a glass slide coated on the bottom side with a thin ITO layer. Incidence angles on the prism and on the ITO layer are explicitly shown. (c) Photograph of the GAU.

A Bruker Vertex 80V Fourier Transform Infrared spectrometer (FTIR) equipped with a tungsten source (operation bandwidth, 330 – 10000 nm), a calcium fluoride beamsplitter (250 – 10000 nm) and two detectors, a Si diode (400 – 1111 nm) and an InGaAs diode (800 – 1724 nm), was used.

All measurements were performed with a grazing angle unit attached to the FTIR sample cavity. This unit consists of two concave mirrors whose angular positions are controlled independently with a computer. With this unit, the incidence and transmission angles can be selected independently and, thus, the angular response in reflection can be accurately obtained. The incident polarization is selected by means of a linear polarizer.

The reflected power in the Kretschmann configuration of Fig. 1 can be simulated with the well-known plane wave method for a one-dimensional multilayer waveguide [13]. The analytical expressions can be found in [4]. On the basis of this method, it is possible to calculate numerically the propagation of light by analysing the reflected power  $R(\theta, \lambda)$  as a function of the angle of incidence and considering the complete set of angles with the following expression [10-12]:

$$T(\lambda) = \frac{\int_{\theta_c}^{90^\circ} p(\theta_1) R^{N(\theta_1)}(\theta_1, \lambda) d\theta_1}{\int_{\theta_c}^{90^\circ} p(\theta_1) d\theta_1} \quad (1)$$

where  $\theta_c$  is the critical angle,  $\lambda$  is the incidence wavelength,  $\theta_1$  is the incidence angle,  $N(\theta_1)$  is the number of reflections at the coating - fiber core interface and  $p(\theta_1)$  is the power distribution of the optical source. A similar method has been validated both for SPRs [2,14] and LMRs [5,6,8].

The broadband light source was modelled as a Gaussian distribution according to [1,8]. Consequently,  $p(\theta_1)$  used in expression (1) is:

$$p(\theta_1) \propto \exp\left[-\frac{(\pi/2 - \theta_1)^2}{2W^2}\right] \quad (2)$$

where  $\theta_1$  is the incidence angle and  $W$  is a parameter related with the Gaussian beam diameter.

With this formalism, reflection is obtained with a Gaussian source instead of a plane wave source, which agrees better with the experimental setup, where the FWHM of the optical source is 2 mm at normal incidence. However, as the incidence angle increases, the width of the Gaussian beam impinging onto the glass-ITO interface also increases because the beam spreads as it separates progressively from normal incidence.

As indicated above, SPRs with ITO thin-films can be obtained for incidence angles ranging from  $40^\circ$  to  $70^\circ$ , whereas LMRs can be obtained with incident angles between  $80$  and  $90^\circ$ . Therefore, we select two incidence angles. The first one is  $\theta_1 = 63.7^\circ$ , (obtained with the setup of Fig. 1 for an incidence angle on the air-prism interface  $\theta_2 = 40^\circ$ ), and it is located in the range of SPR excitation. The second one is  $\theta_1 = 86.5^\circ$ , (obtained with the setup of Fig. 1 for an incident angle on the air-prism interface  $\theta_2 = 5^\circ$ ), and it is located in the range of LMR excitation.

For the  $86.5^\circ$  case it was obtained numerically that  $W = 0.224$  rad is a best fit to the experimental results. Consequently, in view of the fact that the beam spreads 7.8 times less at  $63.7^\circ$ ,  $W = 0.029$  rad was used in this last case.

In the experimental setup of Fig. 1, a Thorlabs N-BK7 Right Angle Prism with the following characteristics was used: shorter side 10mm, uncoated, with all sides polished to 40-20 scratch dig (a parameter that indicates the allowable defects in a surface), leading to  $9.0+/-0.25$ mm side height after polished.

The wavelength dependence of BK7 glass refractive index was adjusted for the simulations according to the Sellmeier expression [14]:

$$n^2 = 1 + \frac{B_1 \lambda^2}{\lambda^2 - C_1} + \frac{B_2 \lambda^2}{\lambda^2 - C_2} + \frac{B_3 \lambda^2}{\lambda^2 - C_3} \quad (3)$$

with parameters:  $B_1 = 1.03961212$ ,  $B_2 = 0.231792344$ ,  $B_3 = 1.01046945$ ,  $C_1 = 0.00600069867 \mu\text{m}^2$ ,  $C_2 = 0.0200179144 \mu\text{m}^2$ , and  $C_3 = 103.560653 \mu\text{m}^2$ .

The prism lied on a 1 mm thick glass slide coated with an ITO layer on the bottom of thickness 68 nm and sheet resistance 15-25  $\Omega/\text{sq}$ , acquired from Cytodiagnosics. For the characterization of the ITO thin-film an ellipsometer UVISEL with spectral range 0.6-6.5 eV (190 – 2100 nm), an angle of incidence  $70^\circ$ , a spot size 1 mm and Software DeltaPsi2TM (from Horiba Scientific Thin Film Division) was used.

The wavelength dependence of ITO thin-film refractive index and extinction coefficient was obtained with the UVISEL ellipsometer and it is shown in Fig. 2. An index matching liquid of refractive index 1.512 was used for connection between the glass-slide and the prism. All measurements were calibrated using an identical but uncoated glass slide, also from Cytodiagnosics.

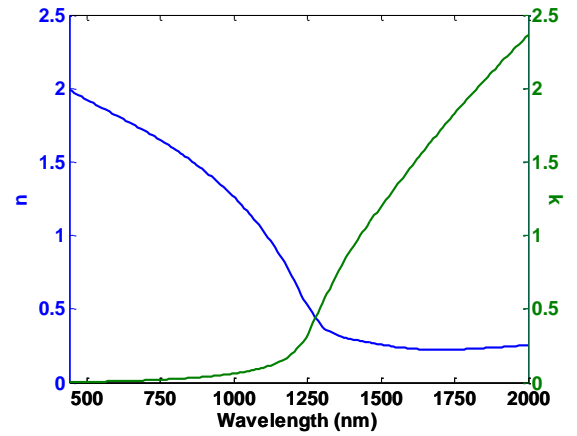


Fig. 2. Index of refraction  $n$  and extinction coefficient  $k$  of ITO deposited thin-film

The numerical results for  $\theta_1 = 63.7^\circ$  are presented in Fig. 3 considering both TE and TM polarization. Likewise, Fig. 4 shows the numerical results corresponding to an incidence angle equal to  $\theta_1 = 86.5^\circ$ .

In Fig. 3 an SPR can be observed for TM polarization at 1395 nm with  $-6$  dB of attenuation, whereas no resonance is observed for TE polarization, in agreement with the known fact that SPRs take place only under TM polarization [4]. In addition to this, the position of the SPR in the optical spectrum at longer wavelengths (1395 nm), agrees with previous works devoted to the analysis of ITO in a Kretschmann configuration [11,12].

Regarding LMRs, according to [5,8] they must be located at shorter wavelengths with an ITO thin-film and they appear both under TM and TE polarization (see the dips at 430 nm and 560 nm respectively). This is exactly what happens in Fig. 4. Moreover, the presence of LMRs for  $86.5^\circ$  (see Fig. 4) and not for  $63.7^\circ$  (see Fig. 3) agrees with the indication in [10] that LMRs with an ITO thin-film must be obtained for angles approaching  $90^\circ$ .

In Fig. 4 an SPR with  $-2$  dB of attenuation can be observed at nearly the same wavelength range as that obtained in Fig. 3. This indicates the wide range of angles able to excite an SPR, though the maximum resonance depth takes place between  $40^\circ$  and  $70^\circ$  [11].

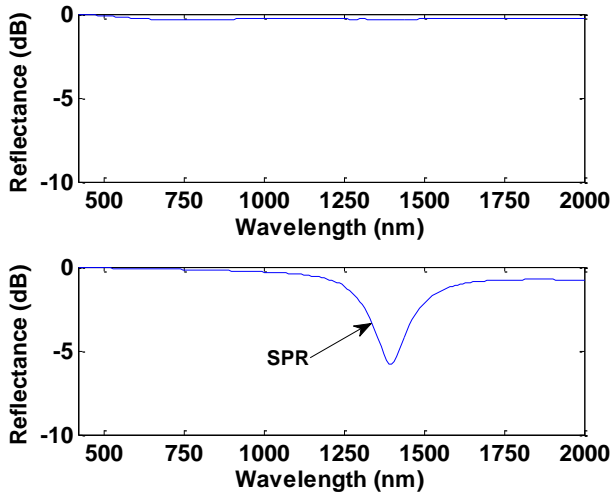


Fig. 3. Theoretical reflection for incidence angle 63.7°: a) TE polarization, b) TM polarization

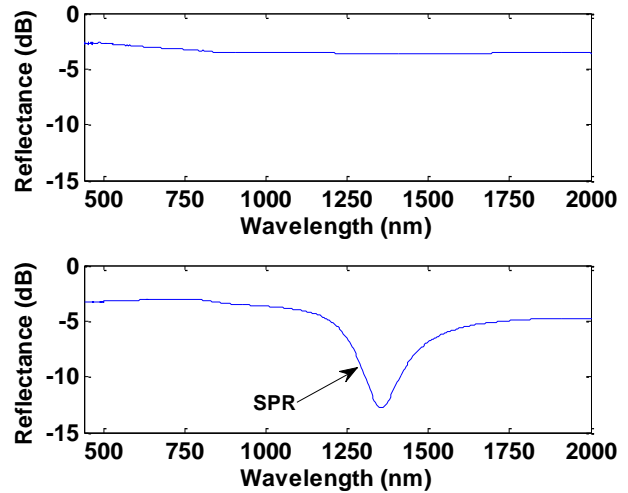


Fig. 5. Experimental reflection for incidence angle 63.7°: a) TE polarization, b) TM polarization

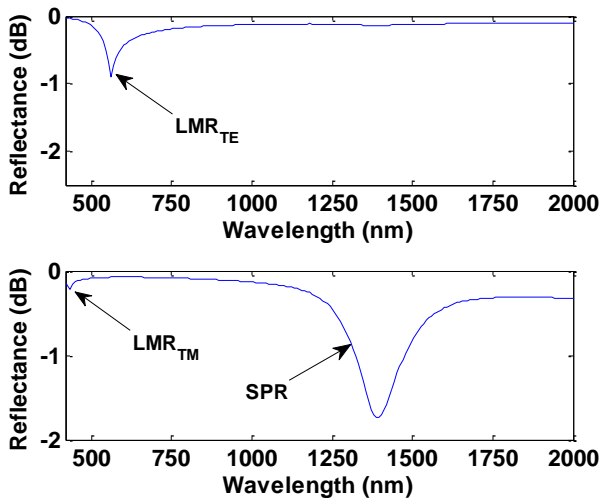


Fig. 4. Theoretical reflection for incidence angle 86.5°: a) TE polarization, b) TM polarization

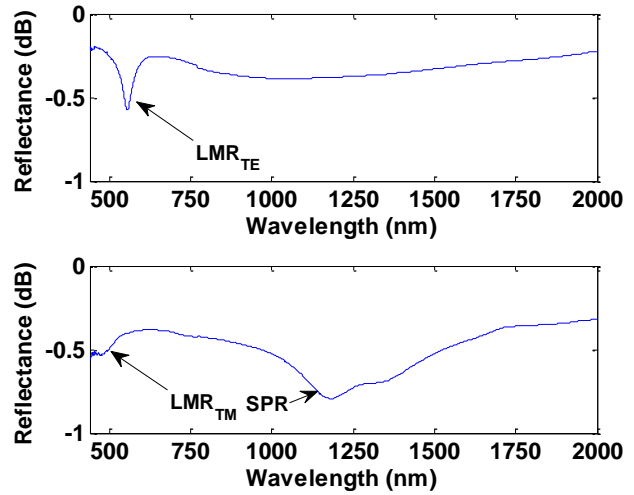


Fig. 6. Experimental reflection for incidence angle 86.5°: a) TE polarization, b) TM polarization

The experimental results corroborating the numerical findings are presented in Fig. 5 and 6. There it can be observed again that the SPR occurs only for TM polarization and that the LMRs can be obtained both for TE and TM polarization for an angle approaching 90°.

For the sake of completeness we show in Fig. 7, the effective index of the mode guided in the thin-film for both TE and TM polarizations as a function of the wavelength. It is noteworthy that the wavelengths where TE and the TM modes start to be guided in the thin-film coincide with those obtained in Fig. 4 and Fig. 6. This demonstrates again the feasibility of obtaining an LMR using both TE and TM polarization.

In Fig. 8 the magnitude of the electric and magnetic vector components of both TE and TM polarization respectively at their cutoff wavelengths 428 nm and 560 nm is shown. For this calculation, it has been assumed that the ITO layer is embedded between two semi-infinite media, namely, air and BK7. The plots show clearly that the penetration depth of the  $E_x$  component is 104 nm, indicating that these devices are adequate for detection of chemical and biological species with size typically below this value.

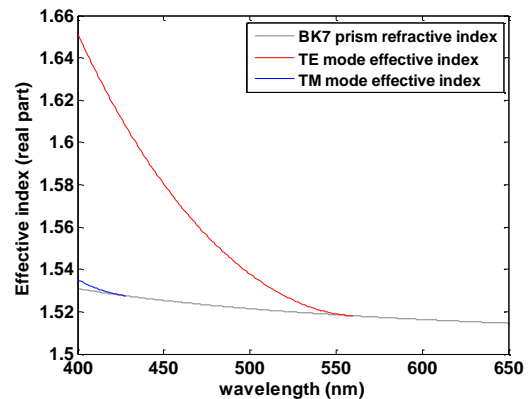


Fig. 7. Effective index of TE and TM modes guided in the ITO thin-film. The refractive index of BK7 prism (dotted line) is included for comparison

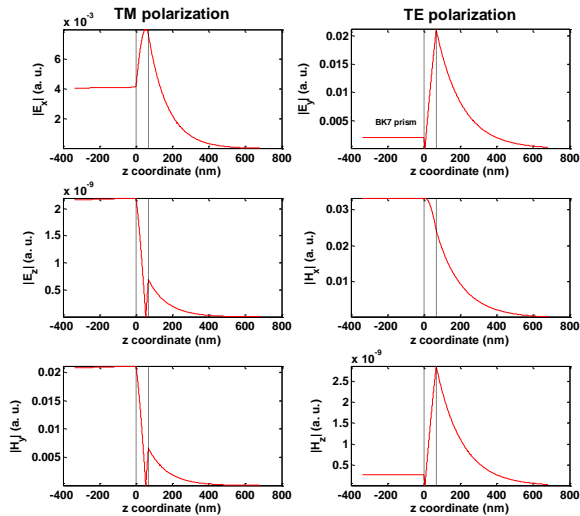


Fig. 8. Vector components of the electric and magnetic field (as a function of the position in the  $z$  axis of Fig. 1), for the mode guided in the thin film: left side TM polarization, right side TE polarization. Negative values of  $z$ -coordinate correspond to the BK7 glass slide and prism region. The vertical dashed lines delimit the region of the ITO layer of thickness 68 nm. Above this layer a semi-infinite air medium is considered.

To conclude, the results presented demonstrate experimentally the generation of both SPRs and LMRs with an ITO thin-film in a Kretschmann configuration by changing the angle of incidence of the light source. Two angles of incidence, namely  $63.7^\circ$  and  $86.5^\circ$ , adequate for an optical generation of an SPR and an LMR respectively, were used in the experiments and in the simulations. The results obtained show that it is possible to obtain an LMR both for TM and TE polarization (at 430 and 560 nm in the optical spectrum respectively), whereas the SPR is only obtained for TM polarization at 1395 nm. The SPR can be observed for both angles of incidence. However, its depth increases at  $63.7^\circ$ , which agrees with the optimal range for SPR generation [1]. On the other hand, the LMR is only visible at  $86.5^\circ$ , which agrees with the range of angles approaching  $90^\circ$  indicated in [10].

The possibility of obtaining both resonances with the same set-up is possible because ITO is a hybrid material that behaves like a metal at longer wavelengths and a non-metallic nature for shorter wavelengths. This indicates that the setup presented in this work expands enormously the type of materials that can be used for the thin-film including both non-metallic (adequate for LMR generation) and metallic (adequate for SPR generation) substrates. Moreover, the different properties of both types of resonances indicated at the beginning of this work will provide the final user with a flexible toolbox to select the best configuration for a specific application. In view of the success obtained in important domains such as the biosensors market with the SPR phenomenon in a Kretschmann configuration, the ideas presented here should contribute to increase the number of applications and the quality of the devices fabricated with this setup.

**Acknowledgment.** This work was supported in part by the Spanish Ministry of Education and Science under contracts FEDER TEC2013-43679-R, CSD2008-00066 and TEC2011-28664-C02. The FTIR spectrometer was financed by the Spanish Ministry of Economy and Competitiveness in the frame of the project CEI10-2-2005. M. Beruete acknowledges funding by the Spanish Government under the research contract program Ramón y Cajal RYC-2011-08221. Special thanks to Horiba Scientific, Thin Film Division for the spectrometric ellipsometry characterization of the samples.

## References

1. R. C. Jorgenson and S. S. Yee, *Sensors Actuators B Chem.* 12, 213 (1993).
2. A. K. Sharma and B. D. Gupta, *Opt. Commun.* 245, 159 (2005).
3. J. Homola, *Chem. Rev.* 108, 462 (2008).
4. J. Homola, *Surface Plasmon Resonance Based Sensors* (Springer, 2006).
5. I. Del Villar, C. R. Zamarreño, M. Hernaez, F. J. Arregui, and I. R. Matias, *J. Light. Technol.* 28, 111 (2010).
6. I. Del Villar, M. Hernaez, C. R. Zamarreño, P. Sánchez, C. Fernández-Valdivielso, F. J. Arregui, and I. R. Matias, *Appl. Opt.* 51, 4298 (2012).
7. D. Kaur, V. K. Sharma, and a. Kapoor, *Sensors Actuators, B Chem.* 198, 366–376 (2014).
8. I. Del Villar, C. R. Zamarreño, P. Sanchez, M. Hernaez, C. F. Valdivielso, F. J. Arregui, and I. R. Matias, *J. Opt.* 12, 095503 (2010).
9. F. Yang and J. R. Sambles, *J. Mod. Opt.* 44, 1155 (1997).
10. I. Del Villar, C. R. Zamarreño, M. Hernaez, P. Sanchez, F. J. Arregui, and I. R. Matias, *Opt. Laser Technol.* 69, 1 (2015).
11. C. Rhodes, S. Franzen, J. P. Maria, M. Losego, D. N. Leonard, B. Laughlin, G. Duscher, and S. Weibel, *J. Appl. Phys.* 100, 54905 (2006).
12. C. Rhodes, M. Cerruti, a. Efremenko, M. Losego, D. E. Aspnes, J. P. Maria, and S. Franzen, *J. Appl. Phys.* 103, 1–6 (2008).
13. P. Yeh, A. Yariv, and C.-S. Hong, *J. Opt. Soc. Am.* 67, 423 (1977).
14. Y. Xu, N. Jones, J. Fothergill, and C. Hanning, "Analytical estimates of the characteristics of surface plasmon resonance fibre-optic sensors," *J. Mod. Opt.* 47, 1099 (2000).

## References (extended version)

1. R. C. Jorgenson and S. S. Yee, "A fiber-optic chemical sensor based on surface plasmon resonance," *Sensors Actuators B Chem.* 12, 213–220 (1993).
2. A. K. Sharma and B. D. Gupta, "On the sensitivity and signal to noise ratio of a step-index fiber optic surface plasmon resonance sensor with bimetallic layers," *Opt. Commun.* 245, 159–169 (2005).
3. J. Homola, "Surface plasmon resonance sensors for detection of chemical and biological species," *Chem. Rev.* 108, 462–493 (2008).
4. J. Homola, *Surface Plasmon Resonance Based Sensors* (Springer, 2006).
5. I. Del Villar, C. R. Zamarreño, M. Hernaez, F. J. Arregui, and I. R. Matias, "Lossy mode resonance generation with indium-tin-oxide-coated optical fibers for sensing applications," *J. Light. Technol.* 28, 111–117 (2010).
6. I. Del Villar, M. Hernaez, C. R. Zamarreño, P. Sánchez, C. Fernández-Valdivielso, F. J. Arregui, and I. R. Matias, "Design rules for lossy mode resonance based sensors," *Appl. Opt.* 51, 4298–4307 (2012).
7. D. Kaur, V. K. Sharma, and a. Kapoor, "High sensitivity lossy mode resonance sensors," *Sensors Actuators, B Chem.* 198, 366–376 (2014).
8. I. Del Villar, C. R. Zamarreño, P. Sanchez, M. Hernaez, C. F. Valdivielso, F. J. Arregui, and I. R. Matias, "Generation of lossy mode resonances by deposition of high-refractive-index coatings on uncladded multimode optical fibers," *J. Opt.* 12, 095503 (2010).
9. F. Yang and J. R. Sambles, "Determination of the optical permittivity and thickness of absorbing films using long range modes," *J. Mod. Opt.* 44, 1155–1164 (1997).
10. I. Del Villar, C. R. Zamarreño, M. Hernaez, P. Sanchez, F. J. Arregui, and I. R. Matias, "Generation of Surface Plasmon Resonance and Lossy Mode Resonance by thermal treatment of ITO thin-films," *Opt. Laser Technol.* 69, 1–7 (2015).
11. C. Rhodes, S. Franzen, J. P. Maria, M. Losego, D. N. Leonard, B. Laughlin, G. Duscher, and S. Weibel, "Surface plasmon resonance in conducting metal oxides," *J. Appl. Phys.* 100, 54905 (2006).
12. C. Rhodes, M. Cerruti, a. Efremenko, M. Losego, D. E. Aspnes, J. P. Maria, and S. Franzen, "Dependence of plasmon polaritons on the thickness of indium tin oxide thin films," *J. Appl. Phys.* 103, 1–6 (2008).
13. P. Yeh, A. Yariv, and C.-S. Hong, "Electromagnetic propagation in periodic stratified media I General theory," *J. Opt. Soc. Am.* 67, 423 (1977).
14. Y. Xu, N. Jones, J. Fothergill, and C. Hanning, "Analytical estimates of the characteristics of surface plasmon resonance fibre-optic sensors," *J. Mod. Opt.* 47, 1099–1110 (2000).